

Implementing the Koopman-von Neumann approach on continuous-variable photonic quantum computers

Xinfeng Gao*, Olivier Pfister†, Stefan Bekiranov‡
University of Virginia, Charlottesville, VA, 22904, USA

The Koopman-von Neumann (KvN) formalism recasts classical mechanics in a Hilbert space framework using complex wavefunctions and linear operators, akin to quantum mechanics. Instead of evolving probability densities in phase space (as in Liouville's equation), KvN uses a Schrödinger-like equation for a classical wavefunction, with commuting position and momentum operators. Mapped to quantum computing, KvN offers a promising route to simulate classical dynamical systems using quantum algorithms by leveraging unitary evolution and quantum linear algebra tools, potentially enabling efficient classical-to-quantum mappings without invoking full quantum uncertainty. In this work, we specifically explore the implementation of the KvN approach on continuous-variable photonic quantum computing architectures, with the goals of leveraging quantum simulation for both sampling and computing intractable nonlinear dynamics. We will demonstrate its implementation and feasibility with two problems: the harmonic oscillator and a 1D partial differential equation governing nonlinear dynamics.

I. Introduction

THE Koopman von Neumann (KvN) formalism offers the prospect of quantum advantage for quantum simulation of classical nonlinear dynamics. The KvN formalism retains the classical phase space, that is, the use of classical variables—position x and momentum p and the phase space structure of classical mechanics, but uses wavefunctions and operators to describe dynamics in a linear, Hilbert space setting. In doing so, KvN enables the use of spectral theory and functional analysis tools traditionally reserved for quantum systems, allowing for deeper insights into classical dynamics. Moreover, it provides a unified language to bridge classical and quantum mechanics, facilitating studies of quantum-classical correspondence, decoherence, and the emergence of classicality. KvN is also particularly valuable in the analysis of long-term behavior and chaos, where Koopman operators serve as a rigorous tool for studying ergodic properties and the spectral characteristics of classical systems.

In this paper, we explore mapping the KvN formula onto continuous-variable quantum computing (CVQC) platforms. Our overarching goal is to develop practical quantum algorithms that are capable of simulating nonlinear nonequilibrium gas kinetics. As an intermediate goal, we will investigate realizable and efficient approaches for mapping the continuous solution variables using quomodes onto a quantum computer. Specifically, we will demonstrate our approach with the Korteweg–De Vries (KdV) equation, describing 1D nonlinear dispersive nondissipative waves.

II. Background and Methodology

A. Derivation of the KvN Formalism

The KvN formalism was initially formulated in terms of classical Liouvillian mechanics but can be cast in a more general form [1–3] that is of direct interest to our approach of using CVQC to simulate classical dynamics. Consider the following, arbitrary ODE

$$\dot{\mathbf{u}} := \frac{d\mathbf{u}}{dt} = \mathbf{v}(\mathbf{u}), \quad (1)$$

where $\mathbf{u}(t) \in \mathbb{R}^{2n}$ are phase space variables with n being the degrees of freedom and \mathbf{v} is an arbitrary vector field [1] which can be generally thought of as nonlinear functions of \mathbf{u} . Notably, Eq. (1) includes Hamilton's equations of

*Professor, Department of Mechanical and Aerospace Engineering, x.gao@virginia.edu, and AIAA Associate Fellow.

†Professor, Department of Physics and Charles L. Brown Department of Electrical and Computer Engineering, opfister@virginia.edu

‡Professor, Department of Biochemistry and Molecular Genetics, sb3de@virginia.edu

motion as well as non-Hamiltonian dynamics such as the KdV equation. Importantly, \mathbf{u} can represent any physical or mathematical dynamical variables as long as their dynamics is described by Eq. (1). We provide an approach to simulating both classes of classical dynamic equations. Similar to Cochran et al. [3] in the case of Hamiltonian dynamics, we will define u_1, u_2, \dots, u_n to be the generalized position coordinates, which are usually defined as q_1, q_2, \dots, q_n , and conjugate momenta as $u_{n+1}, u_{n+2}, \dots, u_{2n}$, which are usually defined as p_1, p_2, \dots, p_n , for a $2n$ -dimensional phase space. Using this definition of the phase space coordinates, Hamilton's equations of motion are

$$\dot{u}_i = \frac{\partial H(\mathbf{u}(t), t)}{\partial u_{n+i}} \quad (2)$$

$$\dot{u}_{n+i} = -\frac{\partial H(\mathbf{u}(t), t)}{\partial u_i}, \quad (3)$$

for $i = 1, 2, \dots, n$. Eqs. (2) and (3) define the relationship between velocity and momentum and Newton's second law, respectively. Defining the phase space variables in this way, Eqs. (2) and (3) clearly take the form of Eq. (1). Note that we will define a momentum operator \mathbf{P} and detail it below.

Without loss of generality, one can define a probability density in phase space $\rho(\mathbf{u}, t)$ which satisfies the continuity equation

$$\frac{\partial \rho(\mathbf{u}, t)}{\partial t} + \nabla \cdot (\mathbf{v}\rho(\mathbf{u}, t)) = 0, \quad (4)$$

where \mathbf{v} is the vector field associated with a conserved quantity (e.g., mass in the case of fluid dynamics or phase space density in the case of Hamiltonian dynamics), and the expectation of any observable $O(\mathbf{u}, t)$, including the phase space vector, \mathbf{u} , is

$$\langle O(\mathbf{u}, t) \rangle = \int O \rho(\mathbf{u}, t) d\mathbf{u}. \quad (5)$$

The first step in deriving the KvN dynamical equations is to define a KvN wavefunction or probability amplitude, $\psi(\mathbf{u}, t)$, in the position representation in terms of the probability density, just as in the case of quantum mechanics [1]

$$\rho(\mathbf{u}, t) = \psi(\mathbf{u}, t)\psi^*(\mathbf{u}, t). \quad (6)$$

Substituting Eq. (6) into Eq. (4) and applying the time and spatial derivatives enables the separation of the result into two self-consistent equations

$$\frac{\partial \psi(\mathbf{u}, t)}{\partial t} = -\left(\frac{1}{2}\psi(\mathbf{u}, t)\nabla \cdot \mathbf{v} + (\mathbf{v} \cdot \nabla)\psi(\mathbf{u}, t)\right), \quad (7)$$

and the complex conjugate of Eq. (7). We can rewrite this equation in the following Schrödinger equation-like form by allowing the first del operator to act on $\psi(\mathbf{u}, t)$ as well as \mathbf{v} and multiplying both sides by $i\hbar$

$$i\hbar \frac{\partial \psi(\mathbf{u}, t)}{\partial t} = \frac{-i\hbar}{2} (\nabla \cdot \mathbf{v} + \mathbf{v} \cdot \nabla) \psi(\mathbf{u}, t), \quad (8)$$

where we note for clarity that the del operator in the first term on the right acts on both \mathbf{v} and $\psi(\mathbf{u}, t)$. The second major step in deriving the KvN formalism is to define a momentum operator $\mathbf{P} = -i\hbar\nabla$ and a position operator $\mathbf{Q} = \mathbf{u}$. Thus, using these operator definitions, we arrive at the KvN equation which takes a Schrödinger equation form [1]

$$i\hbar \frac{\partial \psi(\mathbf{Q}, t)}{\partial t} = H_{\text{KvN}}\psi(\mathbf{Q}, t), \quad (9)$$

where

$$H_{\text{KvN}} = \frac{1}{2} [\mathbf{P} \cdot \mathbf{v}(\mathbf{Q}) + \mathbf{v}(\mathbf{Q}) \cdot \mathbf{P}] \quad (10)$$

is the KvN Hamiltonian operator which is Hermitian. Given that the momentum and position operators are defined in the same way as they are in the standard formulation of quantum mechanics, they satisfy the well known position-momentum commutation relations

$$[Q_i, P_j] = i\hbar\delta_{ij}, \quad (11)$$

where δ_{ij} is the Kronecker delta function (i.e., 1 if $i = j$ and 0 otherwise). Finally, the time evolution of the KvN wavefunction is given by a solution of Eq. (9) in ket form which yields the well known unitary time evolution operator

$$|\psi(t)\rangle = e^{-iH_{\text{KvN}}t/\hbar} |\psi(0)\rangle, \quad (12)$$

from which the Heisenberg equation of motion may be derived

$$\dot{\mathbf{Q}} = \frac{1}{i\hbar} [\mathbf{Q}, H_{\text{KvN}}] = \mathbf{v}(\mathbf{Q}), \quad (13)$$

where we have used Eqs. (10) and (11) to arrive at the final equality. We note that this demonstrates that the KvN formalism is self consistent in that Eq. (13) is the original classical equation of motion Eq. (1) [1]. In summary, this equation describes the evolution, under the KvN Hamiltonian, of a $2n$ -partite quantum system simulating the classical system described by Eq. (1).

In the particular case of quantum optics, $Q_j = (a_j + a_j^\dagger)/\sqrt{2}$ and $P_j = i(a_j^\dagger - a_j)/\sqrt{2}$ are the amplitude and phase quadratures of qumode j of the quantum optical field, a_j and a_j^\dagger being the photon annihilation and creation operators for qumode j . We have the canonical commutation relations $[Q_j, P_k] = i\delta_{jk}$, yielding the Heisenberg inequalities $\Delta Q_j \Delta P_j \geq 1/2$.

In the next section, we show how to leverage quantum optics technology to propose concrete photonic implementations of KvN Hamiltonians.

B. Quantum Algorithm

A practical quantum simulator implementing a KvN Hamiltonian can then be employed to quantum sample Eq. (1), starting from a well-defined initial state $\mathbf{u}(t=0) = \mathbf{u}_o$. Running the quantum KvN circuit and measuring \mathbf{Q} at different times t yields two applications:

- 1) The generation of simulated classical data by quantum sampling of \mathbf{Q} over a probability distribution of \mathbf{u} .
- 2) The computation of $\mathbf{u}(t) = \langle \mathbf{Q}(t) \rangle$ [2].

III. KvN numerical case studies and proposed CVQC experiments

We will consider several test problems: the simple harmonic oscillator, its extension to many coupled oscillators, leveraging the inherent scalability of quantum optics, and the more challenging nonlinear KdV equation.

A. Single harmonic oscillator

We first consider an extremely simple system in order to showcase the KvN formalism and a fully fledged quantum photonics implementation for simulating nanomechanics.

1. General KvN formalism

Using the variables that define the generalized coordinate and conjugate momentum variables as shown in Eqs. (2) and (3), the Hamiltonian of the simple classical harmonic oscillator (HO)

$$H = \frac{1}{2m}u_2^2 + \frac{1}{2}m\omega_o^2u_1^2, \quad (14)$$

where u_1 and u_2 denote the classical position and momentum, respectively, and, using Eqs. (2) and (3), the equations of motion are

$$\dot{u}_1 = \frac{1}{m}u_2 \quad (15)$$

$$\dot{u}_2 = -m\omega_o^2u_1. \quad (16)$$

The KvN approach to this toy problem consists in assigning a quantum mode (qumode) $Q_{1,2}$ for each of the classical variables $u_{1,2}$. We therefore seek Heisenberg equations of the form

$$\dot{Q}_1 = \frac{1}{m}Q_2 \quad (17)$$

$$\dot{Q}_2 = -m\omega_o^2Q_1, \quad (18)$$

which are obtained from the *two-mode* KvN Hamiltonian for a single oscillator, Eq. (10), and the commutation relation, Eq. (11),

$$H_{SO} = \frac{1}{m} P_1 Q_2 - m\omega^2 Q_1 P_2, \quad (19)$$

where Q_j and P_j are now *quantum* position and momentum operators. Note that, while replacing u_1 with Q_1 poses no problem, replacing u_2 with Q_2 does entail a dimension change and dimensional analysis of Eq. (19) shows that m has become homogeneous to a time, while ω_o remains homogeneous to a frequency. In simulation practice, the numerical values of these parameters m and ω_o will not change from the initial physical ones, only the units may change. We will note another important unit change in a moment.

As was proposed in Ref. [3], this KvN-HO Hamiltonian can be formally implemented by a Trotter-Suzuki expansion of two controlled-X gates $[CX_{12}(\alpha) := \exp(-i\alpha Q_1 P_2)]$,

$$e^{-i\frac{\tau}{\hbar} H_{SO}} \simeq \left[e^{-i\frac{\tau}{\hbar} \frac{1}{pm} P_1 Q_2} e^{i\frac{\tau}{\hbar} \frac{m\omega^2}{p} Q_1 P_2} \right]^P. \quad (20)$$

We now propose a new, easier method for implementing this by use of quantum optics.

2. Photonic CVQC KvN implementation

Gaussian (Wigner function) quantum optics readily provides usable quadratic Hamiltonians, namely the beam splitter (BS)

$$H_{BS} = i\hbar\alpha(a_1 a_2^\dagger - a_1^\dagger a_2) \quad (21)$$

$$= \hbar\alpha(P_1 Q_2 - Q_1 P_2), \quad (22)$$

e.g. a partially reflecting mirror, and the two-mode squeezer (TMS)

$$H_{TMS} = i\hbar\beta(a_1^\dagger a_2^\dagger - a_1 a_2) \quad (23)$$

$$= \hbar\beta(P_1 Q_2 + Q_1 P_2), \quad (24)$$

e.g. an optical parametric amplifier based on stimulated (rather than spontaneous) photon pair emission, say in a nonlinear optical material. Using the identity

$$\gamma P_1 Q_2 + \delta Q_1 P_2 = \frac{\gamma+\delta}{2}(P_1 Q_2 + Q_1 P_2) + \frac{\gamma-\delta}{2}(P_1 Q_2 - Q_1 P_2), \quad (25)$$

we rewrite H_{SO} in Eq. (19) as

$$H_{SO} = \frac{\hbar}{2} \left(\frac{1}{m} - m\omega^2 \right) (P_1 Q_2 + Q_1 P_2) + \frac{\hbar}{2} \left(\frac{1}{m} + m\omega^2 \right) (P_1 Q_2 - Q_1 P_2), \quad (26)$$

where we have renormalized the canonical operators Q_j , P_j to quantum optical fields, namely:

$$Q \mapsto \frac{Q}{\beta}, \quad (27)$$

$$P \mapsto \hbar\beta P, \quad (28)$$

with $\beta = (m\omega/\hbar)^{1/2}$. (Note that β plays no role in H_{SO} as $PQ \mapsto \hbar PQ$). This renormalization of operators lets us define the photon annihilation operator as $a = (Q + iP)/\sqrt{2}$, $a^\dagger a$ being the *dimensionless* photon number operator.

3. Quantum optical implementation

The new form of H_{SO} in Eq. (26) lets us write the Trotter-Suzuki expansion of H_{SO} as

$$e^{-i\frac{\tau}{\hbar} H_{SO}} \simeq \left[e^{-i\frac{\tau}{2p} (\frac{1}{m} - m\omega^2)(P_1 Q_2 + Q_1 P_2)} e^{-i\frac{\tau}{2p} (\frac{1}{m} + m\omega^2)(P_1 Q_2 - Q_1 P_2)} \right]^P, \quad (29)$$

which corresponds to the sequencing of a two-mode squeezer with a beamsplitter, respectively. Note that these two building blocks can Trotterize any Gaussian Hamiltonian. Such quantum optical Trotterization was demonstrated

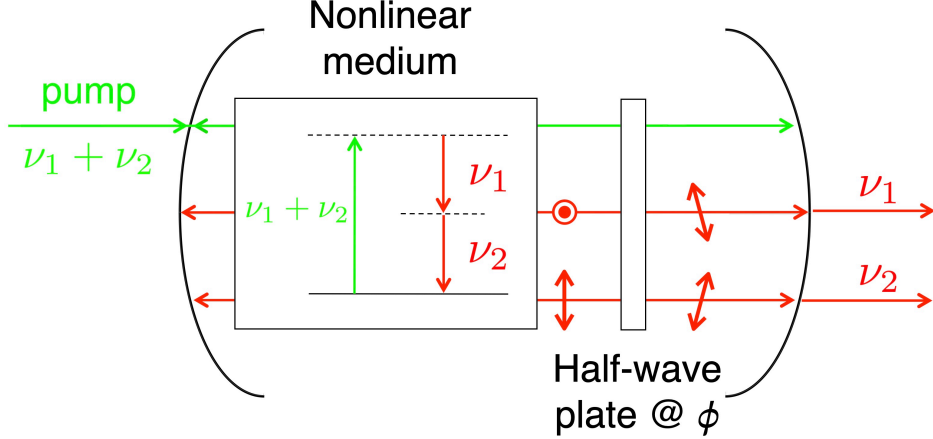


Fig. 1 Principle sketch of a Trotterizing optical parametric oscillator for the simulation of a classical harmonic oscillator. The OPO signal fields (qumodes 1 and 2 in the text) are embodied by OPO modes with orthogonal linear polarizations. The “type-II” OPO nonlinear medium on the left (e.g. KTP or PPKTP) annihilates pump photons of frequency $\nu_p = \nu_1 + \nu_2$ to create pairs of orthogonally polarized signal photons at ν_1 and ν_2 . The corresponding fields are then mixed by a half-wave plate at orientation ϕ equivalently to a beam splitter of angle $\theta = 4\phi$ (see text). For illustration, the field polarizations are sketched qualitatively going left to right in the initial round trip. Each round trip inside the OPO cavity constitutes a Trotter-Suzuki step in Eq. (29).

experimentally, to a very good approximation, by one of us (OP) on two different TMS gates in the first-ever large-scale cluster-state entanglement of an optical frequency comb [4, 5]. The procedure is to place the aforementioned gates (TMS, BS) inside a resonant optical cavity. Additional compactness can be achieved by encoding the two qumodes in polarization rather than space and using a half-wave plate, as depicted in Fig. 1. The device in Fig. 1 is a type-II optical parametric oscillator (OPO), constituted by a resonant optical cavity which effectively implements the p Trotter steps over p round trips (on average). The OPO cavity contains a nonlinear optical crystal, such as periodically poled KTiOPO_4 (i.e., Potassium Titanyl Phosphate), which two-mode-squeezes the two qumodes 1 and 2 by photon-pair emission. In Fig. 1, the qumodes are orthogonally polarized and a half-wave plate acts as a variable beam splitter. The intensity of the pump beam in the nonlinear crystal and the wave plate angle provide two independent controls for precisely adjusting the Trotter parameters $\frac{1}{m} \mp m\omega^2$ in Eq. (26).

Let’s now examine the simulation regimes that are accessible experimentally. Let us define r to be the squeezing parameter of the OPO. For an OPO below the oscillation threshold, over p passes, we have

$$Q_1 - Q_2 \mapsto e^r (Q_1 - Q_2) \quad (30)$$

$$P_1 - P_2 \mapsto e^{-r} (P_1 - P_2) \quad (31)$$

with $r = 1.15$ for a 10 dB squeezing ratio. We thus have

$$\frac{r}{p\tau} = \frac{1}{2} \left(\frac{1}{m} - m\omega_o^2 \right). \quad (32)$$

The beam splitter field reflectivity can be expressed as $\rho = \cos \theta$ and we have

$$\frac{\theta}{\tau} = \frac{1}{2} \left(\frac{1}{m} + m\omega_o^2 \right). \quad (33)$$

This yields the simulated oscillator parameters

$$m = \tau \left(\theta + \frac{r}{p} \right)^{-1}, \quad (34)$$

$$\omega_o = \frac{1}{\tau} \left(\theta^2 - \frac{r^2}{p^2} \right)^{\frac{1}{2}}. \quad (35)$$

Taking typical OPO parameter values $\tau = 1$ ns, $r = \pm 1$, $\theta = 0.1$ rad, yields $m \sim 10^{-9}$ kg and $\omega_o/2\pi \sim 0.1$ GHz, i.e., a nanomechanical oscillator.

B. Coupled harmonic oscillator network

We now extend this implementation to a network of coupled oscillators. This could be used in the context of a recent quantum algorithm proposed for the exponentially faster simulation of coupled oscillators [6].

1. KvN Formalism

Using the generalized coordinates and conjugate momentum variables defined in Eqs. (2) and (3), the classical Hamiltonian of n coupled oscillators is

$$H_{CO}^{(\text{class.})} = \sum_{j=1}^n \left(\frac{u_{n+j}^2}{2m_j} + \frac{\kappa_j}{2} u_j^2 \right) + \sum_{j=1}^n \sum_{k>j} \kappa_{jk} (u_j - u_k)^2 \quad (36)$$

$$= \sum_{j=1}^n \left(\frac{u_{n+j}^2}{2m_j} + \frac{\xi_j}{2} u_j^2 \right) + \sum_{j=1}^n \sum_{k\neq j} \xi_{jk} u_j u_k \quad (37)$$

where $\xi_{jk} = -2\kappa_{jk} = \xi_{kj}$ and $\xi_j = \kappa_j + \sum_{k\neq j} \kappa_{jk}$. Following the KvN formalism, we promote $\mathbf{u} = (u_1, \dots, u_{2n})^T$ to a position operator, $\mathbf{Q} = (Q_1, \dots, Q_{2n})^T$. Using Eq. (13), the Heisenberg equations are

$$\dot{\mathbf{Q}} = \begin{pmatrix} & & & \frac{1}{m_1} & & & \\ & & & & \frac{1}{m_2} & & \\ & & & & & \ddots & \\ & & & & & & \frac{1}{m_n} \\ -\xi_1 & -\xi_{12} & \dots & -\xi_{1n} & & & \\ -\xi_{12} & -\xi_2 & \dots & -\xi_{2n} & & & \\ \vdots & \vdots & \ddots & \vdots & & & \\ -\xi_{1n} & -\xi_{2n} & \dots & -\xi_n & & & \end{pmatrix} \mathbf{Q}, \quad (38)$$

where the blank entries in the matrix are zeroes. Using Eq. (10), the $2n$ -mode KvN Hamiltonian is therefore, including Trotterization options:

$$H_{CO} = \underbrace{\sum_{j=1}^n \frac{1}{m_j} P_j Q_{j+n} - \sum_{j=1}^n \xi_j P_{j+n} Q_j}_{\text{independent oscillators (TMS+BS)}} - \underbrace{\sum_{j=1}^n \sum_{k\neq j} \xi_{jk} P_{j+n} Q_k}_{\text{coupling graph (TMS only)}}. \quad (39)$$

2. Quantum photonic implementation

As for the single harmonic oscillator, the KvN Hamiltonian can be Trotterized using beamsplitters and squeezers inside an optical cavity. Here, the platform advantage we seek is scalability: the more oscillators, the more interesting the simulation. Previous research by one of us (OP) demonstrated that one can make use of the spectral degree of freedom offered by the quantum optical frequency comb (QOFC) of resonant OPO modes as an eminently scalable platform for quantum computing [7]. In particular, entanglement of as many as 60 qumodes into a cluster state, a quantum computing “substrate,” has been experimentally demonstrated [4, 8].

The design challenges will consist here in, (i), employing frequency-domain beamsplitters [green term in Eq. (39)] and, (ii), implementing the arbitrary coupling matrix, $(\xi_{jk})_{j,k}$ [blue term in Eq. (39)], needed for the simulation at hand. While addressing specific designs are out of the scope of this paper, we wish to point out that sophisticated QOFC engineering methods have already been proposed, based on optical phase modulation [9] as well as on generation of arbitrary entanglement graphs [10, 11]. These results will be applied to specific oscillator coupling topologies as needed.

C. Korteweg-De Vries equation

We now turn to a more arduous, nonlinear simulation problem, the Korteweg-De Vries equation, which models waves on a shallow water surface.

1. KvN formalism

The 1D KdV equation of a function $u(x, t)$ has the form

$$\frac{\partial u}{\partial t} - 6u \frac{\partial u}{\partial x} + \frac{\partial^3 u}{\partial x^3} = 0. \quad (40)$$

This problem is chosen for its dispersive and nonlinear properties, representing typical features in fluid dynamics. In a first step, we convert the PDE of Eq. (40) to an ODE, using a finite difference method on the 1D grid of pitch Δx with a periodic boundary in x , as shown in Fig. 2, to yield the discretized Eq. (41). Note that the discretization scheme is not

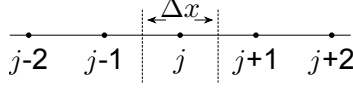


Fig. 2 Control volume in 1D.

restricted to finite differences. Methods such as finite volume, finite element, or Galerkin are applicable.

$$\frac{du_j}{dt} = v_j(u) \equiv -\frac{3}{\Delta x}(u_{j+1}^2 - u_{j-1}^2) - \frac{1}{2\Delta x^3}(u_{j-2} - 2u_{j-1} + 2u_{j+1} - u_{j+2}). \quad (41)$$

Equation (41) will lend itself well to KvN implementation provided one has access to non-Gaussian quantum gates. From Eq. (10), we obtain the corresponding KdV-KvN Hamiltonian

$$H_{\text{KdV}} = \underbrace{-\frac{1}{2\Delta x^3} \sum_{j=1}^N (P_j Q_{j-2} - 2P_j Q_{j-1} + 2P_j Q_{j+1} - P_j Q_{j+2})}_{\text{Gaussian Hamiltonian } H_G \text{ (BS only)}} - \underbrace{\frac{3}{\Delta x} \sum_{j=1}^N (P_j Q_{j+1}^2 - P_j Q_{j-1}^2)}_{\text{non-Gaussian Hamiltonian } H_{NG}}. \quad (42)$$

2. Photonic CVQC implementation

As for the harmonic oscillator case, we now proceed to implement the KdV-KvN Hamiltonian on a photonic quantum machine, again using a Trotter-Suzuki expansion.

- 1) Remarkably, close examination of the Gaussian term H_G on the RHS of Eq. (42) in light of Eq. (21) reveals that it solely contains beamsplitter terms—of field reflectivities $\cos(\tau/(2\Delta x^3))$ and $\cos(\tau/(\Delta x^3))$, where τ is the fixed propagation time through the beamsplitter—and can therefore simply be viewed as an N -mode optical interferometer.
- 2) The term H_{NG} corresponds to the difficult, nonlinear part of the calculation, and can be termed a controlled-squeezing term, i.e., qumodes $j \pm 1$ being squeezed by a value determined by the field in qumode j . Such cubic gates can be implemented using alternating Gaussian two-mode squeezers (in blue) and non-Gaussian single-mode cubic phase gates (in red) [12]

$$e^{i3\alpha t P_j Q_k^2} = e^{i2\alpha Q_j Q_k} e^{i t P_j^3} e^{-i\alpha Q_j Q_k} e^{-i t P_j^3} e^{-i2\alpha Q_j Q_k} e^{i t P_j^3} e^{i\alpha Q_j Q_k} e^{-i t P_j^3} e^{i \frac{3}{4} \alpha^3 t Q_j^3}. \quad (43)$$

However, such a complicated gate decomposition does not necessarily need to be implemented directly. One of us (OP) recently discovered that non-Gaussian cubic phase gates such as $\exp(iP_j^3)$ can be directly and quasi-deterministically prepared by use of reinforcement learning (RL) [13]: a neural network can be trained to drive the quantum optical circuit of Fig. 3 and produce cubic-phase states $\exp(i\alpha Q^3)|0\rangle_p = \int ds \exp(i\alpha s^3)|s\rangle_q$, which can in turn implement single-mode cubic-phase gates $\exp(i\alpha Q^3)$ deterministically by (Gaussian) quantum teleportation [14]. Extension of this research to two-mode cubic phase gates such as the LHS of Eq. (43) is underway.

Another, fascinating avenue of research involves Trotterization of all components in a single OPO: note that Fig. 3 describes the generation of a standalone cubic phase state $\exp(i\alpha Q^3)|0\rangle_p$ with full strength α , whereas the quantum circuit Trotterizing Eq. (42) only requires strength α/p for p Trotter steps. The idea will therefore be to extend our RL approach to combining all Trotterization components and yield the quantum evolution governed by Eq. (42). A very preliminary, but initially much more feasible, experimental implementation could be to approximate the quantum evolution from Eq. (42) with $\exp(-i\frac{\tau}{\hbar} H_G) \exp(-i\frac{\tau}{\hbar} H_{NG})$, i.e., a $2n$ -mode interferometer fed by cubic phase states.

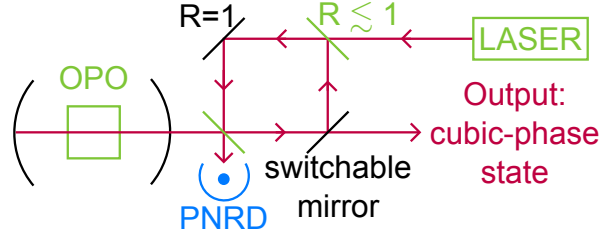


Fig. 3 Optical circuit for generating a cubic phase state. PNRD: photon-number-resolving detector. The components in green (OPO squeezing parameter, beamsplitter reflectivity, laser intensity) are controlled by the neural network, whose input data is from the components in blue (PNRD). The square delay loop also acts as an optical memory when the state is ready, in order to synchronize all such circuits, by switching all reflectivities to 1. The switchable mirror (e.g., Mach-Zehnder interferometer) allows the prepared state to continue to the rest of the circuit when ready.

Once the whole KvN Hamiltonian of Eq. (42) is implemented, all we have to do is measure the amplitude quadratures $\{Q_j\}_{j=1,\dots,N}$ at the circuit's output. The measurement averages will yield the classical solutions $u_j = \langle Q_j \rangle$. Note that the initial state $u(t=0)$ can be encoded straightforwardly using displacement operations such as the one realized by the laser in Fig. 3.

IV. Concluding Remarks and Future Work

The KvN formalism embeds classical dynamics in a Hilbert space using unitary evolution, enables simulation of classical systems with quantum algorithms, and facilitates use of quantum linear algebra to extract dynamical features of classical systems. One open question is that of reachable quantum advantage when simulating a classical system with a quantum machine. While the KvN formalism provides a systematic way to do this, one should remember that the mathematical problem space for an N -body classical system in 3 spatial dimensions, e.g. N coupled oscillators, is the $6N$ -dimensional phase space of all position and momentum components, whereas the mathematical problem space for an N -qubit quantum system is the exponentially vaster 2^N -dimensional Hilbert space of all quantum states. This remark constitutes the original case for quantum simulation made by Feynman [15]. Beyond these dimensionality considerations, one can argue that a quantum machine could be beneficial when the classical computation is really hard, as in the case of a highly nonlinear Hamiltonian like the KdV one above. Other cases of interest might include nonintegrable classical and quantum systems. All these may provide interesting directions of investigation if the quantum machine can simulate faster than a classical machine can calculate, as quantum sampling and reconstructing expectation values on a full-scale quantum machine could be expected to be faster than classical numerics. Finally, one should also weigh the important advances of photonic quantum computing which can be leveraged in this context [7].

References

- [1] Joseph, I., “Koopman–von Neumann approach to quantum simulation of nonlinear classical dynamics,” *Phys. Rev. Res.*, Vol. 2, 2020, p. 043102. <https://doi.org/10.1103/PhysRevResearch.2.043102>, URL <https://link.aps.org/doi/10.1103/PhysRevResearch.2.043102>.
- [2] Barthe, A., Grossi, M., Tura, J., and Dunjko, V., “Continuous Variables Quantum Algorithm for Solving Ordinary Differential Equations,” *2023 IEEE International Conference on Quantum Computing and Engineering (QCE)*, Vol. 02, 2023, pp. 48–53. <https://doi.org/10.1109/QCE57702.2023.10183>.
- [3] Cochran, S., Stokes, J., Jayakumar, P., and Veerapaneni, S., “An application of continuous-variable gate synthesis to quantum simulation of classical dynamics,” *AVS Quantum Science*, Vol. 7, No. 2, 2025, p. 023801. <https://doi.org/10.1116/5.0234007>, URL <https://doi.org/10.1116/5.0234007>.
- [4] Pysher, M., Miwa, Y., Shahrokhsahi, R., Bloomer, R., and Pfister, O., “Parallel generation of quadripartite cluster entanglement in the optical frequency comb,” *Phys. Rev. Lett.*, Vol. 107, No. 3, 2011, p. 030505. <https://doi.org/10.1103/PhysRevLett.107.030505>.
- [5] Miller, J. L., “Entanglement gets scaled up in an optical frequency comb,” *Physics Today*, Vol. 64, No. 9, 2011, p. 21. URL <https://doi.org/10.1063/PT.3.1243>.

- [6] Babbush, R., Berry, D. W., Kothari, R., Somma, R. D., and Wiebe, N., “Exponential Quantum Speedup in Simulating Coupled Classical Oscillators,” *Phys. Rev. X*, Vol. 13, 2023, p. 041041. <https://doi.org/10.1103/PhysRevX.13.041041>, URL <https://link.aps.org/doi/10.1103/PhysRevX.13.041041>.
- [7] Pfister, O., “Continuous-variable quantum computing in the quantum optical frequency comb,” *Journal of Physics B: Atomic, Molecular and Optical Physics*, Vol. 53, No. 1, 2020, p. 012001. <https://doi.org/10.1088/1361-6455/ab526f>, URL <https://doi.org/10.1088/1361-6455/ab526f>.
- [8] Chen, M., Menicucci, N. C., and Pfister, O., “Experimental realization of multipartite entanglement of 60 modes of a quantum optical frequency comb,” *Phys. Rev. Lett.*, Vol. 112, 2014, p. 120505. <https://doi.org/10.1103/PhysRevLett.112.120505>, URL <http://link.aps.org/doi/10.1103/PhysRevLett.112.120505>.
- [9] Zhu, X., Chang, C.-H., González-Arciniegas, C., Pe’er, A., Higgins, J., and Pfister, O., “Hypercubic cluster states in the phase-modulated quantum optical frequency comb,” *Optica*, Vol. 8, No. 3, 2021, pp. 281–290. <https://doi.org/10.1364/OPTICA.411713>, URL <http://www.osapublishing.org/optica/abstract.cfm?URI=optica-8-3-281>.
- [10] Wang, P., Chen, M., Menicucci, N. C., and Pfister, O., “Weaving quantum optical frequency combs into hypercubic cluster states,” *Phys. Rev. A*, Vol. 90, 2014, p. 032325. URL <http://dx.doi.org/10.1103/PhysRevA.90.032325>.
- [11] Brunel, L., Klich, I., Pe’er, A., and Pfister, O., “Theoretical analysis of the spectrally pumped quantum optical frequency comb,” *in preparation*, 2025.
- [12] Kalajdzievski, T., and Arrazola, J. M., “Exact gate decompositions for photonic quantum computing,” *Phys. Rev. A*, Vol. 99, 2019, p. 022341. <https://doi.org/10.1103/PhysRevA.99.022341>, URL <https://link.aps.org/doi/10.1103/PhysRevA.99.022341>.
- [13] Anteneh, A., Brunel, L., González-Arciniegas, C., and Pfister, O., “Deep reinforcement learning for near-deterministic preparation of cubic- and quartic-phase gates in photonic quantum computing,” [arXiv:2506.07859 \[quant-ph\]](https://arxiv.org/abs/2506.07859), 2025.
- [14] Gottesman, D., Kitaev, A., and Preskill, J., “Encoding a Qubit in an Oscillator,” *Phys. Rev. A*, Vol. 64, 2001, p. 012310.
- [15] Feynman, R. P., “Simulating Physics With Computers,” *Int. J. Theor. Phys.*, Vol. 21, 1982, pp. 467–488.